no interaction between cations and anions in solution ("free ions").

There are two observations that might shed some light on the problem. The first is that below $R = 4$ precipitation of material occurs in the triethylmethylammonium system and is rapid below $R = 3.5$. This may be an indication that tetracyanocobaltate(II), which was implicated in the mechanism of decomposition earlier, is ion-paired quite differently relative to those systems using other counterions. The second point is that at $R = 5$ solutions are yellow when the cation is triethylmethylammonium and not green. This is best interpreted as a change in the equilibrium constant favoring less dissociation of the pentacyanocobaltate complex. It is unfortunate that infrared measurements cannot resolve this matter since pentacyanocobaltates show weak bands in the region 2110–2090 cm^{-1} and thus it becomes difficult to assess $[Co(CN)_5]^{3-}$:$[Co(CN)_4]^{2-}$ ratios accurately when the former ion is in large excess. There are clearly some subtle nuances between the behavior of the triethylmethylammonium system and those employing other counterions that cannot be detected by infrared spectroscopy but perhaps might be resolved by extensive conductivity measurements.

On the basis of the presented data, a switch from acetonitrile to DMF might eliminate the problem with the cyanation reaction when the counterion is PNP, K-crown, or Bu_4N. Indeed, reaction starts to occur when the solvent composition is 1:1 DMF-d_7/acetonitrile-d_3 for the K-crown system at 45 °C. Since in some situations DMF may present a problem in workup, the original combination of acetonitrile and triethylmethylammonium cation still remains the best choice for the cyanation reaction.

Acknowledgment is made to the donors of the Petroleum Research Fund, administered by the American Chemical Society, and to the National Science Foundation (Grant CHE-8209006) for support of the research. We thank Allyn McIntyre for the preparation of the figures.

Registry No. $(PNP)_2[Co(CN)_4]\cdot 4DMF$, 102746-96-3; $Li_3[Co(CN)_5]$, 24803-72-3; $[Co(CN)_5]^{3-}$, 14971-18-7; $[Co(CN)_4]^{2-}$, 18901-67-2; $[Co(CN)_3(CH_3CN)]^-$, 38141-16-1; $[Co(CN)_3(DMF)]^-$, 102746-97-4; $Co(CN)_2(CH_3CN)_2$, 38141-15-0; $Co(CN)_2(DMF)_2$, 102746-98-5; PNP^+, 48236-06-2; Bu_4N^+, 10549-76-5; K-crown$^+$, 31270-13-0; Li^+, 17341-24-1; $Li_3[Co(CN)_5H]$, 24803-73-4; Et_3MeN^+, 302-57-8; isocrotyl chloride, 513-37-1.

Supplementary Material Available: Tables of hydrogen atom atomic coordinates, temperature factors, and nonessential bond lengths and angles (5 pages). Ordering information is given on any current masthead page.

Contribution from the Department of Chemistry,
Texas A&M University, College Station, Texas 77843

Deprotonation of $[HMo(CO)_2(P^\frown P)_2]BF_4$ Complexes: Hard Anions as Proton Carriers

Marcetta Y. Darensbourg* and Maria M. Ludvig

Received December 12, 1985

Reported are kinetic studies of the deprotonation of $[HMo(CO)_2(P^\frown P)_2]BF_4$ complexes ($P^\frown P$ = 1,2-bis(diphenylphosphino)ethane, dppe; $P^\frown P$ = 1,2-bis(dimethylphosphino)ethane, dmpe; $P^\frown P$ = 1,2-bis(diethylphosphino)ethane, depe). Amine bases deprotonated the metalloacids slowly, $t_{1/2}$ typically being days, following the rate expression rate = $k_2[MoH^+][amine]$. Deprotonation rates were dependent on the size of the amine bases and were greatly enhanced by the addition of salts of hard anions such as halides and acetate. The rate expression for deprotonation by mixed-base systems loses dependence on [amine], substituting instead a dependence on $[X^-]$. The dependence of rate on the steric and electronic nature of the $P^\frown P$ ligand was interrelated with similar features of the base. Activation energy parameters, H/D kinetic isotope effects, and solvent effects suggest Mo–H bond breaking as well as coordination sphere rearrangement in the transition state.

Introduction

The protonation/deprotonation reactions of transition-metal hydride complexes as well as carbon acids undergo electronic, and hence geometric, changes that are not found in protonation/deprotonation of nitrogen and oxygen acids. Heterolytic cleavage of an M–H bond generating M^- and H^+ requires an oxidation state change of two units for each. Although this formal view exaggerates the actual changes in charge distributions, the deprotonation of the M–H bond involves extensive polarization of electron density.

Our studies in this area are based on the well-known $HMo(CO)_2(P^\frown P)_2^+$ cations. Earlier we reported the X-ray crystal structure of $HMo(CO)_2(dppe)_2^+$ (**1H$^+$** (dppe = 1,2-bis(diphenylphosphino)ethane) as its $AlCl_4^-$ salt and suggested the unlocated hydride ligand to be in or near the girdle of a pentagonal bipyramid, largely flanked by phenyl rings of the dppe ligands.[1] Consistent with this view, rates of deprotonation by amine bases (pyridine, py; NEt_3; $NHEt_2$) were very slow and were found to be greatly enhanced upon addition of salts of small hard anions such as F^- and Cl^-. The hypothesis was advanced that the small, largely unsolvated anion assisted $Mo–H^+$ bond cleavage by its ability to penetrate the outer coordination sphere of **1H$^+$**, polarize the hydride ligand toward H^+ in a preamble to H-bonding, and carry the proton to the amine base. To further examine this claim, we have extended studies of $HMo(CO)_2(P^\frown P)_2^+$ deprotonation, varying the steric and electronic nature of $P^\frown P$, as well as studying solvent effects and H/D kinetic isotope effects.

Experimental Section

Materials. All solid reagents and ligands were obtained from standard vendors and used as received. The acid $HBF_4\cdot Et_2O$ (Aldrich) and 1,8-diazabicyclo[5.4.0]undec-7-ene (DBU, Aldrich; see Table II footnotes for formula) were sealed with a septum and stored under a positive pressure of argon. Bis(triphenylphosphine)nitrogen(1+) acetate (PPN^+OAc^-), PPN^+F^-, and PPN^+I^- were synthesized by ion exchange with PPN^+Cl^- as described in the literature.[2] All solvents and bases were distilled under N_2 from appropriate drying agents (THF, Na^0/benzophenone; CH_2Cl_2, P_2O_5; $Me_2C{=}O$, $MgSO_4$; CH_3CN, CaH_2 followed by P_2O_5; Me_2SO, py, NEt_3, and lutidene (2,6-dimethylpyridine), BaO) and degassed with argon before use.

Preparation. The $[HMo(CO)_2(P^\frown P)_2^+]BF_4^-$ (**1H$^+$**BF_4^-, $P^\frown P$ = 1,2-bis(diphenylphosphino)ethane, dppe; **2H$^+$**BF_4^-, $P^\frown P$ = 1,2-bis(dimethylphosphino)ethane, dmpe) salts were synthesized as previously described by substituting HBF_4 as protonating agent and recrystallizing from CH_2Cl_2/Et_2O.[3,4] The 1,2-bis(diethylphosphino)ethane (depe) derivative (**3H$^+$**) was prepared in a manner similar to the case of the dppe derivative. That is, $Mo(N_2)_2(depe)_2$ was synthesized according to the method of George and Noble[5] and converted to $Mo(CO)_2(depe)_2$ (**3**) following the same procedure as described for $Mo(CO)_2(dppe)_2$. The

---

(1) Hanckel, J. M.; Darensbourg, M. Y. *J. Am. Chem. Soc.* **1983**, *105*, 6979.

(2) Martinsen, A.; Songstad, J. *Acta Chem. Scand. Ser. A* **1977**, *A31*, 615.

(3) Datta, S.; McNeese, T. J.; Wreford, S. S. *Inorg. Chem.* **1977**, *16*, 2661.

(4) Connor, J. A.; Riley, P. I.; Rix, C. J. *J. Chem. Soc., Dalton Trans.* **1977**, 1317.

(5) George, T. A.; Noble, M. E. *Inorg. Chem.* **1978**, *17*, 1678.

0020-1669/86/1325-2894$01.50/0

Table I. Spectral Characterization of $Mo(CO)_2(P\frown P)_2$ and $[HMo(CO)_2(P\frown P)]BF_4$[a]

$P\frown P$	IR[b] ν_{CO}, cm^{-1}	^1H NMR[b,c] δ (t of t)	J_{P-H}, Hz	$J_{P'-H}$, Hz	$J_{H-^{13}C}$, Hz
trans-**1**	1822				
cis-**1**	1851 s, 1781 s				
1H$^+$	1983 vw, 1879 s	−5.2	89	14	
(^{13}CO)-**1H**$^+$	1938 vw, 1839 s				
trans-**2**	1815[d]				
cis-**2**	1836 s, 1766 s				
2H$^+$	1975 vw, 1872 s	−6.4[e]	69	8.4	
trans-**3**	1777				
cis-**3**	1827 s, 1755 s				
3H$^+$	1965 vw, 1862 s	−6.85	70	9.2	
(^{13}CO)-**3H**$^+$	1921 w, 1821 s	−6.76[e]	69.6	9.0	4.4

$P\frown P$	IR[b] ν_{CO}, cm^{-1}	^2H NMR[b,c] δ (t of t)	J_{P-H}, Hz	$J_{P'-H}$, Hz
1D$^+$	1879 s	−5.4	11	1
2D$^+$	1871 s	−6.6	11	1

[a] $P\frown P$ = dppe, **1** and **1H**$^+$; $P\frown P$ = dmpe, **2** and **2H**$^+$; $P\frown P$ = depe, **3** and **3H**$^+$. [b] CH_2Cl_2 or CD_2Cl_2 solution spectra except where noted. [c] Hydride region only. [d] Hexane solution. [e] Acetone-d_6.

deep yellow THF solution of $Mo(CO)_2(depe)_2$ was filtered through Celite and the volume reduced. Hexanes were added, yielding a small amount of pink solid, and the yellow solution was filtered through a glass frit. Following unsuccessful attempts to obtain **3** as a solid, a molar excess of $HBF_4 \cdot Et_2O$ was added to a CH_2Cl_2 solution of **3**. Solvent was removed, and the yellow solid $[HMo(CO)_2(depe)_2^+]BF_4^-$, **3H**$^+BF_4^-$, was recrystallized from THF/hexane. Anal. (Galbraith Labs). Found (calcd): C, 39.06 (40.50); H, 7.29 (7.59).

Deuterated samples were prepared by adding a solution of $D_2O/HBF_4 \cdot Et_2O$ (3:1 v/v D_2O to HBF_4) to neutral dicarbonyls. **1D**$^+BF_4^-$ and **2D**$^+BF_4^-$ were obtained as solids as described above. The percent deuterium was assessed by ^1H NMR. The integration-derived ratio of the (residual) ^1H hydride resonance in **1D**$^+$ to selected protons on the ligand were compared to the analogous ratio determined for all-protio **1H**$^+$ and **2H**$^+$. The deuterium level was 90% for **1D**$^+$ and 70% for **2D**$^+$.

Kinetics Measurements. Reactions monitored with time were carried out in 25-mL Schlenk tubes, capped with rubber septa, from which samples were periodically withdrawn by syringe and measured by IR. Temperature control was maintained in a constant-temperature bath. For higher temperature reactions, samples were withdrawn at intervals, placed in degassed septa-capped tubes, and quenched at −78 °C. Samples from these tubes were later (within 6 h) analyzed by FTIR. Rates of reaction were monitored over 1–2 half-lives by following the disappearance of the intense $\nu(CO)$ IR absorption of the $[HMo(CO)_2(P\frown P)_2^+]BF_4^-$ species (Table I), in the presence of excess base. Observed rate constants (k_{obsd}) were calculated with a linear-least-squares program for the first-order rate plots of ln $(A_t - A_\infty)$ vs. time. For the kinetic isotope effect studies, the k_{obsd} value for **1D**$^+$ was corrected for the residual **1H**$^+$ present by assuming the observed rate constant was the weighted average of independent **1H**$^+$ and **1D**$^+$ contributions.

Results and Discussion

The great similarities in the $\nu(CO)$ IR and ^1H NMR data (Table I) indicate the solution structures of **1H**$^+$, **2H**$^+$, and **3H**$^+$ to be consistent with the structure of $HMo(CO)_2(dppe)_2^+$ as determined by X-ray analysis.[1] The very intense absorption in the region of 1862–1879 cm^{-1} has been assigned to the asymmetric stretch of CO groups trans to each other.[6,7] The very weak band at higher energies, 1965–1983 cm^{-1}, has not been previously reported. In order to confidently assign this band to the $\nu(CO)$ symmetric vibration, the CO stretching force constants , k_t and k_i, werre calculated by the Cotton–Kraihanzel method[8] from the observed $\nu(CO)$ frequencies of **1H**$^+$ and **3H**$^+$. The values of k_t are 15.06 and 14.8/ mdyn/Å, and the values of k_i are 0.8037 and 0.7959 mdyn/Å for **1H**$^+$ and **3H**$^+$, respectively. From the calculated k_t and k_i values, the band positions for the ^{13}CO analogue of **1H**$^+$ and **3H**$^+$ were calculated at 1938 cm^{-1}, A′, and 1837 cm^{-1}, A″, for $Mo(^{13}CO)_2(dppe)_2H^+$ and 1921 cm^{-1}, A′, and 1821 cm^{-1}, A″, for $Mo(^{13}CO)_2(depe)_2H^+$. The ^{13}CO-labeled complexes were prepared, and the observed $\nu(CO)$ frequencies (Figure 1, Table I) are in excellent agreement with these calculations.

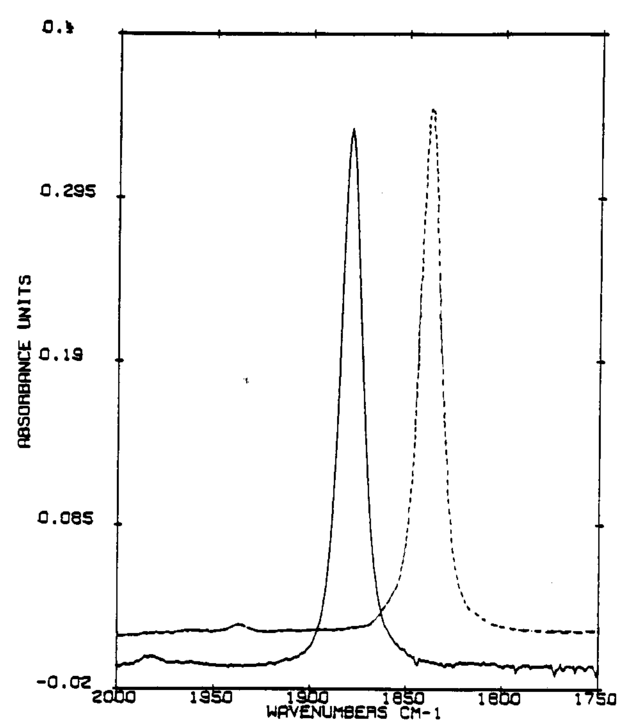

Figure 1. $\nu(CO)$ spectra of $[HMo(^{12}CO)_2(dppe)_2^+]BF_4^-$ (—) and $[HMo(^{13}CO)_2(dppe)_2^+]BF_4^-$ (- - -) in THF solution.

The assignment of the very weak band was important to this project because the relative intensities, $I_{A'}$ and $I_{A''}$, of the two $\nu(CO)$ bands can be related to the angle θ between the local oscillating dipoles of the CO groups according to eq 1.[9] The

$$I_{A''}/I_{A'} = \tan^2 (\theta/2) \qquad (1)$$

$I_{A'}/I_{A''}$ ratio was determined from the spectrum in Figure 1 to be 9.09 × 10^{-3} for **1H**$^+$, corresponding to θ = 169°, similar to the 175° angle of (OC)–Mo–(CO) established in the solid state. Cations **2H**$^+$ and **3H**$^+$ have very similar intensity ratios and therefore similar geometries.

Earlier Datta, McNeese, and Wreford studied the stereochemical changes associated with the deprotonation of **1H**$^+$ and **2H**$^+$.[3] The kinetic product of deprotonation is *trans*-**1** and *trans*-**2** (eq 2). A subsequent unimolecular isomerization to the thermodynamically more stable isomers *cis*-**1** and *cis*-**2** occurs. Similar observations were made in our work. The most reactive deprotonating agent for the three metalloacids was KO-*t*-Bu and in all cases produced almost within time of mixing the trans isomer of the conjugate base, which could be observed to convert to the cis isomer on standing. Less active deprotonating agents showed rates of deprotonation similar to or slower than the isomerization rate.

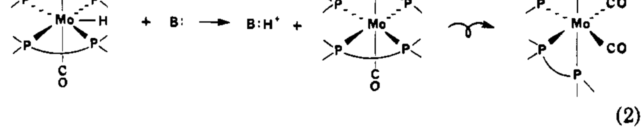

(2)

The $\nu(CO)$ frequencies of **1H**$^+$, **2H**$^+$, and **3H**$^+$ reflect the electron-donating capability of the $P\frown P$ ligands: dppe < dmpe < depe. The enhanced electron density at the Mo along this series is also manifest in the observed acidity: **1H**$^+$ > **2H**$^+$ > **3H**$^+$. For example, a 25-fold excess of py deprotonates **1H**$^+$ to the extent

---

(6) Datta, S.; Dezube, B.; Kouba, J. K.; Wreford, S. S. *J Am. Chem Soc.* **1978**, *100*, 4404.

(7) Bond, A. M.; Colton, R.; Jackowski, J. J. *Inorg. Chem.* **1975**, *14*, 2526.

(8) Cotton, F. A.; Kraihanzel, C. S. *J. Am. Chem. Soc.* **1962**, *84*, 4432.

(9) Braterman, P. S. *Metal Carbonyl Spectra*; Academic: New York, 1975.

of 45% of equilibrium (requiring 5 days beyond which time no further changes were observed as determined by examining the ν(CO) bands in the FTIR). In contrast, there was no observable deprotonation of **2H**$^+$ or **3H**$^+$ by py over extended periods.

Earlier we observed both a kinetic and thermodynamic promotion of deprotonation of **1H**$^+$BF$_4^-$ by py in the presence of Cl$^-$.[1] Equations 3 and 4, which show the percent yields measured after equilibrium was established as described above, indicate that both py and chloride deprotonate **1H**$^+$BF$_4^-$ incompletely. Concerted addition of the two reagents however resulted in 100% deprotonation (eq 5). The shift is understood to be due to an enhanced ion-pair interaction of Cl$^-$ with the hard proton site on the pyH$^+$ ion in eq 5 as compared to all other possible ionic interactions. The equilibrium constants for eq 3, 4, and 5, respectively, are given as

$$\mathbf{1}\mathrm{H^+BF_4^-} + \mathrm{py} \xrightleftharpoons[\mathrm{CH_2Cl_2}]{5\ \mathrm{days},\ 30\ ^\circ\mathrm{C}} \underset{45\%}{\mathbf{1}} + \mathrm{pyH^+BF_4^-} \tag{3}$$

$$\mathbf{1}\mathrm{H^+BF_4^-} + \mathrm{PPN^+Cl^-} \xrightleftharpoons[\mathrm{CH_2Cl_2}]{5\ \mathrm{h},\ 30\ ^\circ\mathrm{C}} \underset{20\%}{\mathbf{1}} + \mathrm{PPN^+BF_4^-} + \mathrm{HCl} \tag{4}$$

$$\mathbf{1}\mathrm{H^+BF_4^-} + \mathrm{PPN^+Cl^-} + \mathrm{py} \xrightarrow[\mathrm{CH_2Cl_2}]{5\ \mathrm{h},\ 30\ ^\circ\mathrm{C}} \underset{100\%}{\mathbf{1}} + \mathrm{pyH^+Cl^-} + \mathrm{PPN^+BF_4^-} \tag{5}$$

$$K_3 = \frac{[\mathbf{1}][\mathrm{pyH^+BF_4^-}]}{[\mathbf{1}\mathrm{H^+BF_4^-}][\mathrm{py}]}$$

$$K_4 = \frac{[\mathbf{1}][\mathrm{PPN^+BF_4^-}][\mathrm{HCl}]}{[\mathbf{1}\mathrm{H^+BF_4^-}][\mathrm{PPN^+Cl^-}]}$$

$$K_5 = \frac{[\mathbf{1}][\mathrm{pyH^+Cl^-}][\mathrm{PPN^+BF_4^-}]}{[\mathbf{2}\mathrm{H^+BF_4^-}][\mathrm{PPN^+Cl^-}][\mathrm{py}]}$$

It can easily be seen that

$$K_5 = \frac{K_4[\mathrm{pyH^+Cl^-}]}{[\mathrm{HCl}][\mathrm{py}]} = K_3\frac{[\mathrm{pyH^+Cl^-}][\mathrm{PPN^+BF_4^-}]}{[\mathrm{PPN^+Cl^-}][\mathrm{pyH^+BF_4^-}]}$$

It follows that K_5 should be greater than K_4 since the term [pyH$^+$Cl$^-$]/[HCl][py] should be greater than 1. The differences between K_5 and K_3 are more subtle. The distinction between the ion pairs are slight, but better contact interactions are expected for the ion pairs pyH$^+$Cl$^-$ and PPN$^+$BF$_4^-$, thus making $K_5 > K_3$. A similar effect has been observed for the deprotonation of **2H**$^+$BF$_4^-$. In fact, no H$^+$ abstraction by py was observed over a period of 7 days; PPN$^+$F$^-$ established an equilibrium deprotonation of 100% within 10 min, and the mixture of PPN$^+$F$^-$ and py completely deprotonated **2H**$^+$BF$_4^-$ in CH$_2$Cl$_2$ within 1 min.

Another example of kinetic control during the deprotonation of the metalloacids was observed with KOAc solubilized by dibenzo-18-crown-6. The acetate deprotonated completely all three complexes; however, the time required varied widely. The final equilibrium time was reached in 2 min, 4 h, and 17 h for **2H**$^+$, **3H**$^+$, and **1H**$^+$, respectively. This order parallels increasing steric hindrances of the ligands.

The prominent difference in the rate at which equilibrium was established in eq 3–5 above has been further studied. The rate of deprotonation of **1H**$^+$BF$_4^-$ by py in CH$_2$Cl$_2$ showed a first-order dependence both on [**1H**$^+$] and on [py] (entries 1–4, Table II). In the presence of added Cl$^-$ the dependence on [py] was lost (entries 6, 8, and 9) and replaced by a [Cl$^-$] dependence. Hence, the rate law in the absence of anion additives is as shown in eq 6, and that in their presence is given by eq 7.

$$\mathrm{rate} = k_2[\mathbf{1}\mathrm{H^+}][\mathrm{py}] \tag{6}$$

$$\mathrm{rate} = k_2[\mathbf{1}\mathrm{H^+}][\mathrm{anion^-}] \tag{7}$$

In the presence of py and added F$^-$, the rate of deprotonation of **1H**$^+$BF$_4^-$ was too rapid to measure. As entries 10–12 of Table II show, the dependence of deprotonation rate varies: F$^-$ > Cl$^-$ > Br$^-$ > I$^-$. Acetate ion also promotes deprotonation (entry 13), and the value for k_2 is between that of Cl$^-$ and Br$^-$.

As mentioned previously, fluoride ion promotes the deprotonation of **2H**$^+$ by py (entry 17, Table II). In CH$_2$Cl$_2$, the chloride ion does not deprotonate **2H**$^+$ to any appreciable extent. In the absence of Cl$^-$, the dependence of k_{obsd} on [NEt$_3$] is linear and therefore the rate law is similar to eq 6. The addition of 20 equiv of Cl$^-$ enhances the rate of deprotonation of **2H**$^+$ by NEt$_3$ by 1 order of magnitude, and as indicated by entry 21, the dependence on NEt$_3$ concentration is lost in the presence of Cl$^-$.

Entries 24–27 in Table II show the reactivity of the bulky strong base DBU to vary **2H**$^+$ ≫ **1H**$^+$ > **3H**$^+$. The large difference in reactivity of the dmpe vs. the dppe derivative suggests a steric control of the reaction since **1H**$^+$ is by all other indications a stronger acid than is **2H**$^+$. However, the relative order of the other two members of the series, **1H**$^+$ > **3H**$^+$, suggests that electronic factors override the opposing steric factors.

In order to further probe the nature of the transition state of this reaction, deprotonation rates of **1H**$^+$BF$_4^-$ by chloride ion were measured in different solvents. The results were as follows. In CH$_2$Cl$_2$ a 20-fold excess of PPN$^+$Cl$^-$ reacts with **1H**$^+$BF$_4^-$ to achieve the equilibrium expressed in eq 4, 20% deprotonation, within 4–6 h at 30 °C. In Me$_2$SO, the k_{obsd} value is 1.27×10^{-2} min^{-1}; in acetone, $k_{\mathrm{obsd}} = 3.42 \times 10^{-2}$ min^{-1}; and in THF, the reaction proceeds at a rate too rapid for monitoring by our conventional sampling techniques. Thus, the order of dependence of rate on solvent is CH$_2$Cl$_2$ < Me$_2$SO < acetone < THF. Neither solvent dielectric constant (7.3 (THF) < 8.9 (CH$_2$Cl$_2$) < 20.7 (acetone) < 49 (Me$_2$SO)) nor Gutmann donor numbers[10] (undetermined, but very small for CH$_2$Cl$_2$ < 17 (acetone) < 20 (THF) < 30 (Me$_2$SO)) correlated with the observed rate trends. In contrast, acceptor numbers, a measure of the interaction of Et$_3$PO with solvent as determined from ^{31}P chemical shift data, showed somewhat of a correlation: 20.4 (CH$_2$Cl$_2$) < 19 (Me$_2$SO) < 12 (acetone) < 8 (THF).[10] Although the use of acceptor and donor numbers has met with limited success (probably because of their interrelatedness), in this case the correlation with acceptor number satisfactorily agrees with our tentative working model. That is, if the most important aspect of the halide effect is to make close contact with a localized, incipient δ^+ site on HMo(CO)$_2$($\widehat{\mathrm{PP}}$)$_2^+$, then the solvent that would best prevent such interaction or best solvate the Cl$^-$ is expected to produce the slowest rates.

The temperature dependence of deprotonation of **1H**$^+$BF$_4^-$ in CH$_2$Cl$_2$ by pyridine in the presence of Cl$^-$ is shown in Table III. In agreement with the observed bimolecularity of the rate expression $\Delta S^\ddagger$ is negative. The $\Delta H^\ddagger$ value is 16.6 kcal/mol. These values are comparable to the values obtained by Jordan and Norton[11] for the proton exchange of CpM(CO)$_3$H (M = Cr, Mo, W) with CpM(CO)$_3^-$. The $\Delta H^\ddagger$ value is too small to signify any Mo–ligand bond-breaking process. (Gas-phase studies have shown that group 6 M–H homolytic bond energies vary from 35 to 65 kcal/mol;[12] for example diatomic Cr$^+$–H is 35 ± 4 kcal/mol[12a] and (CO)$_6$Mo$^+$–H is 65 ± 3 kcal/mol.[12b] A kinetic measurement of $\Delta H^\ddagger$ for the dissociative process Mo(CO)$_6$ + P(n-C$_4$H$_9$)$_3$ → CO + Mo(CO)$_5$P(n-C$_4$H$_9$)$_3$ was found to be 32 kcal/mol.[13]) A bond-making process or a coupling of bond-making and complex structural/solvent rearrangements is indicated.

Table II also contains rate constants determined for the deprotonation of DMo(CO)$_2$(dppe)$_2^+$ by py in the presence of anion additives. The $k_{\mathrm{H}}/k_{\mathrm{D}}$ ratios are as follows: Cl$^-$, 2.30; Br$^-$, 1.86; OAc$^-$, 1.55. A larger KIE was observed for the deprotonation of **1H**$^+$ vs. **1D**$^+$ by DBU; $k_{\mathrm{H}}/k_{\mathrm{D}} = 3.0$. With KO-$t$-Bu, rates of reaction with both **1H**$^+$ and **1D**$^+$ are too rapid for measurement.

---

(10) Gutmann, V. *The Donor-Acceptor Approach to Molecular Interactions*; Plenum: New York, 1978.

(11) Jordan, R. F.; Norton, J. R. *J. Am. Chem. Soc.* **1982**, *104*, 1255.

(12) (a) Armentrout, P. B.; Halle, L. F.; Beauchamp, J. L. *J. Am. Chem. Soc.* **1981**, *103*, 6501. (b) Stevens, A. E.; Beauchamp, J. L. *J. Am. Chem. Soc.* **1981**, *103*, 190.

(13) Graham, J. R.; Angelici, R. J. *Inorg. Chem.* **1967**, *6*, 2082.

(14) Bell, R. P. In *The Proton in Chemistry*, 2nd ed.; Cornell University Press: Ithaca, NY, 1973; Chapter 11.

Table II. Rates of Deprotonation of $[HMo(CO)_2(P\frown P)_2^+]BF_4^-$ in CH_2Cl_2 Solvent[a]

entry	metalloacid	[metalloacid], M	base	equiv	anion[b]	equiv	k_2,[c] M^{-1} min^{-1}
1	**1H**$^+$	0.004	py	25			$4.14\ (\pm0.38) \times 10^{-3}$
2		0.004	py	35			$3.65\ (\pm0.12) \times 10^{-3}$
3		0.004	py	45			$3.53\ (\pm0.12) \times 10^{-3}$
4		0.004	py	55			$3.55\ (\pm0.15) \times 10^{-3}$
5		0.004	py	20	Cl^-	15	$1.96\ (\pm0.18) \times 10^{-1}$
6		0.004	py	20	Cl^-	22	$1.93\ (\pm0.20) \times 10^{-1}$
7		0.004	py	20	Cl^-	30	$1.98\ (\pm0.08) \times 10^{-1}$
8		0.004	py	5	Cl^-	20	$2.06\ (\pm0.09) \times 10^{-1}$
9		0.004	NEt_3	20	Cl^-	20	$2.01\ (\pm0.01) \times 10^{-1}$
10		0.004	py	20	I^-	20	$1.40\ (\pm0.16) \times 10^{-2}$
11		0.0053	py	20	Br^-	20	$2.40\ (\pm0.10) \times 10^{-2}$
12		0.0063	py	20	OAc^-	20	$1.30\ (\pm0.07) \times 10^{-1}$
13		0.0041	py	20	Cl^-	20	$2.14\ (\pm0.09) \times 10^{-1}$[d]
14	**1D**$^+$	0.0044	py	20	Cl^-	20	$9.29\ (\pm0.44) \times 10^{-2}$
15		0.0052	py	20	Br^-	20	$1.29\ (\pm0.03) \times 10^{-2}$
16		0.0051	py	20	OAc^-	20	$8.40\ (\pm0.38) \times 10^{-2}$
17	**2H**$^+$	0.0074	py	20	F^-	20	immediate
18		0.00798	NEt_3	20			$2.08\ (\pm0.06) \times 10^{-2}$
19		0.0081	NEt_3	42			$1.56\ (\pm0.05) \times 10^{-2}$
20		0.0076	NEt_3	106			$1.16\ (\pm0.03) \times 10^{-2}$
21		0.0074	NEt_3	20	Cl^-	20	$1.97\ (\pm0.20)^i \times 10^{-1}$
		0.0074	NEt_3	49	Cl^-	20	
		0.0074	NEt_3	83	Cl^-	20	
22	**2D**$^+$	0.0065	py	20	F^-	20	$6.18\ (\pm0.09) \times 10^{-1}$[e]
23	**3H**$^+$	0.0061	py	20	F^-	20	$6.22\ (\pm0.12) \times 10^{-2}$
24	**1H**$^+$	0.0051	DBU[h]	20			$5.56\ (\pm0.69) \times 10^{-2}$[g]
25	**1D**$^+$	0.0049	DBU	20			$1.84\ (\pm0.18) \times 10^{-2}$
21	**2H**$^+$	0.0074	DBU	20			*f*
27	**3H**$^+$	0.0061	DBU	20			$3.09\ (\pm0.49) \times 10^{-2}$[g]

[a] Entries 1–10 at 29 ± 1 °C,[1] all others at 31 ± 1 °C. [b] Anion additive added as bis(triphenylphosphine)nitrogen(1+), PPN^+, salt. [c] k_2 is obtained from either k_{obsd}/[base] or k_{obsd}/[anion]; the error is calculated at 90% confidence limit for k_{obsd}. Each deprotonation reaction was performed once, except where noted, and the reproducibility for each individual run is ~10%. All k_2 values for the deuterated complexes have been corrected for the amount of protio complex present. [d] Average of three runs; error is average error. [e] Average of two runs; error is average error. This value cannot be corrected for the amount of **2H**$^+$ present since its value for k_2 cannot be determined by our experimental techniques. [f] Deprotonation was complete with 2 min; estimate $k_2 > 9\ M^{-1}\ min^{-1}$. [g] Average of four runs; error is average error. [h] DBU =

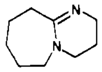

[i] k_2 is the average (error, standard deviation in the average) of three runs. An accurate determination of k_2 is difficult because the reaction proceeds too quickly for accurate determinations of k_{obsd}.

Table III. Temperature Dependence of Rate Constants for Deprotonation of $[HMo(CO)_2(P\frown P)_2^+]BF_4^-$[a]

T, K	k_2,[b] M^{-1} min^{-1}	T, K	k_2,[b] M^{-1} min^{-1}
303.16	$1.91\ (\pm0.05) \times 10^{-1}$	318.16	$8.38\ (\pm0.08) \times 10^{-1}$
304.16	$2.05\ (\pm0.10) \times 10^{-1}$	323.16	$1.24\ (\pm0.10)$
304.16	$2.05\ (\pm0.03) \times 10^{-1}$	328.16	$1.46\ (\pm0.15)$
304.16	$2.17\ (\pm0.07) \times 10^{-1}$		

E_{act} = 17.2 (±1.4) kcal/mol

$\Delta H^* = 16.6\ (\pm1.4)$ kcal/mol

$\Delta S^* = -9.2\ (\pm4.7)$ eu

[a] Deprotonations accomplished with 20 equiv of PPNCl and 20 equiv of py in CH_2Cl_2 solvent. [b] k_2 is obtained from k_{obsd}/[anion]; error is calculated at 90% confidence limit.

Table IV. Deprotonation Reactions of $[HMo(CO)_2(P\frown P)_2^+]BF_4^-$ in CH_2Cl_2: Equilibrium Positions

metalloacid	[metalloacid], M	base	equiv	% deprotonation at equil (time, days)
1H$^+$	0.004	py	25	45 (5 d)
1H$^+$	0.004	NEt_3	25	100 (3 d)
2H$^+$	0.0056	NEt_3	20	100 (1 d)
	0.0056	py	20	0 (5 d)
3H$^+$	0.0061	NEt_3	20	95 (10 d)
	0.0061	NEt_3	75	100 (7 d)

The most obvious reason for the existence of deuterium isotope effects is the difference in the zero-point energies of M–H vs. M–D bonds. The zero-point energy is equal to $^1/_2\ h\nu$ (where h is Planck's constant and ν is the frequency of A–H vibration). If a hydrogen atom is transferred to an acceptor B, the stretching vibration is lost in the transition state. The difference between the amount of energy needed to bring the two complexes to the (linear) transition state will be the difference in the zero-point energies. From the reasonable assumption that $\nu_{M-H} \simeq 2000\ cm^{-1}$, the difference in rate for M–H/M–D would be about fourfold at room temperature and represents the maximum KIE. This method takes into account only the loss of the stretching vibration and is a crude approximation of any real situation. Deprotonation reactions using the strong base DBU have substantial bond breakage in the transition state since the k_H/k_D ratio is close to the calculated maximum. In contrast, the weaker bases, Cl^-, Br^- and OAc^-, have smaller k_H/k_D ratios and therefore suggest a smaller amount of M–H or M–D bond cleavage character in the transition state. The variation in the k_H/k_D ratio with base strength has been noted in the deprotonation of carbon acids in aqueous solution. In such cases the k_H/k_D ratio increases, goes through a maximum at $\Delta pK_a = 0$, and then decreases as the base strength increases.[15] This is true for symmetrical transition states and when and if the bond strength and force constants for AH and BH are the same. For the metalloacids, the maximum will probably occur at some value other than $\Delta pK_a = 0$; however, the trend should be the same.

Conclusions

The rates found for the deprotonation of the metalloacids $HMo(CO)_2(P\frown P)_2^+$ are many magnitudes slower than what would be found for the deprotonation of oxygen or nitrogen acids, which have rates at or near the diffusion control limit. The rates found here are inversely dependent on the size of the X^- base used; i.e., rates decrease in the order $F^- > Cl^- > Br^- > I^-$. Since the basicity of X^- decreases as $F^- > Cl^- > Br^- > I^-$, size and electronic effects are inseparable for X^-.

---

(15) Bell, R. P. In *The Proton in Chemistry*, 2nd ed.; Cornell University Press: Ithaca, NY, 1973; Chapter 12.

Scheme I

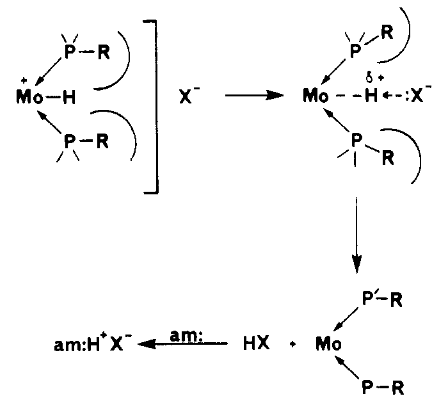

For the neutral amine bases, the rates of deprotonation of $HMo(CO)_2(P\frown P)_2^+$ are primarily dependent on the size, suggesting that the outer ligand sphere must undergo some rearrangement for the amine lone pair to contact the proton (as in $[Mo–H^+\cdots:N]$). There is a marked enhancement of proton transfer to the amine bases in the presence of X^- carriers. The kinetic expression for these mixed-base systems shows no dependence on [N:], but it does depend on $[X^-]$.

There is a complex dependence on the $P\frown P$ ligand involving both steric and electronic factors. The steric environment is reduced in going from $\mathbf{1H}^+$ to $\mathbf{2H}^+$, and this is reflected in the difference in the rate of deprotonation using the strong bulky base DBU. With a smaller base of intermediate strength, py, the electronic factors dominate and the deprotonation of $\mathbf{1H}^+$ (the stronger acid) is faster than for $\mathbf{2H}^+$.

In addition to all the above factors affecting the metalloacid deprotonation rates, solvent dependence is important. The rate of deprotonation of $\mathbf{1H}^+$, using py/Cl^-, depends on the solvent and varies as $CH_2Cl_2 < Me_2SO <$ acetone $<$ THF, spanning a range of at least 2 orders of magnitude. Since the solvent that solvates Cl^- the least produces the fastest rate, we assume this solvation effect to be due to ion-pairing interactions, which vary from solvent to solvent. Jordan and Norton[11] found only a small solvent effect, a factor of 2 between CD_3CN and THF-d_8, for the proton-exchange rate between $CpM(CO)_3H$ and $K[CpM(CO)_3]$ (M = Cr, Mo, W) without the presence of any added small anion carriers.

We suggest that the proton-transfer mechanism of the metalloacids, $HMo(CO)_2(P\frown P)_2^+$, in nonaqueous solvents, has been defined by several probes and that the events are well modeled by Scheme I. An electrostatic interaction of anion with cation precedes coordination sphere rearrangement (in this case most likely a motion of the R substituents on P or an opening of the angle of the P–Mo–P that envelops the Mo–H site) to permit optimum X^- interaction with the acid ($Mo^{\delta+}$–H) site. The polarization of Mo–H bond density required for loss of hydrogen as H^+ is proposed to occur in a linear transition state that has less metal–hydrogen bond breaking than hydrogen–anion bond making. The X^- ion then serves to carry out the proton to its thermodynamic sink, the amine base. The slow rates of these reactions (as compared to orders of magnitude more rapid rates of metalloacids such as $CpM(CO)_3H$ (M = Cr, Mo, W), for example[11]) is, in our view, highly indicative of the large steric encumbrances in $HMo(CO)_2(P\frown P)_2^+$.

Acknowledgment. This work was supported by the Robert A. Welch Foundation. Appreciation is expressed to Dr. J. M. Hanckel, who initiated this project.

Registry No. $\mathbf{1H}^+$, 63765-16-2; $\mathbf{2H}^+$, 102735-00-2; $\mathbf{3H}^+$, 94241-76-6; py, 110-86-1; NEt_3, 121-44-8; DBu, 6674-22-2; Cl^-, 16887-00-6; I^-, 20461-54-5; Br^-, 24959-67-9; OAc^-, 71-50-1; F^-, 16984-48-8; D_2, 7782-39-0.

Notes

Contribution from the Laboratory of Analytical
Chemistry, Faculty of Science, Nagoya University,
Chikusa, Nagoya, 464 Japan

Mechanistic Study on the Complex Formation of Aluminum(III), Gallium(III), and Indium(III) Ions in Dimethyl Sulfoxide and *N*,*N*-Dimethylformamide

Koji Ishihara, Shigenobu Funahashi, and Motoharu Tanaka*

Received November 26, 1985

We have measured the activation volumes for the complexation of iron(III) and nickel(II) ions in aqueous and nonaqueous media.[1,2] The activation volume for complexation of Ni(II) ion is invariably positive, and it does not largely vary with different solvents, so that the mechanism of the ion remains unchanged within the framework of a dissociative interchange in any solvent. On the other hand, in the case of Fe(III) ion, for which the complexation has been proved to proceed via an associative mode of activation in water, the activation volume does vary to a large extent with entering ligands and coordinated solvents. We have concluded, from these findings, that the bulkiness of reactants is reflected to a larger extent in the activation volume for the complexation with an associative character in water than for the complexation with a dissociative character in aqueous solution.

We report in this paper a study on the high-pressure kinetics of the complex formation of aluminum(III), gallium(III), and indium(III) ions in Me_2SO in order to understand more thoroughly the effect of the steric bulkiness of reactants and solvents on the reaction mechanism. Al(III), Ga(III), and In(III) ions with isoelectronic configurations in the same column of the periodic table were chosen because we expect to investigate selectively a size effect of metal ions on complexation.

Experimental Section

Due care was given to moisture and explosion of perchlorates.

Solvents. Dimethyl sulfoxide (Me_2SO) and *N*,*N*-dimethylformamide (DMF) were purified as described previously[2] and were used within a couple of days after purification.

Reagents. Hydrated Aluminum(III) Perchlorate. A 13-g sample of aluminum (99.99%, Wakojunyaku, Osaka, Japan) was dissolved in 200 cm^3 of 60% $HClO_4$ (Super Special grade, Wakojunyaku) diluted with 150 cm^3 of distilled water. Concentration of the solution by gentle evaporation yielded hydrated salts.

Hydrated Gallium(III) Perchlorate. A 7-g portion of shot-shaped gallium (99.99%, Wakojunyaku) was dissolved in a 100 cm^3 of 60% $HClO_4$ by gentle heating.

Hydrated Indium(III) Perchlorate. A 1-g portion of shot-shaped indium (99.98%, Wakojunyaku) in limited amounts was added to 50 g of 60% $HClO_4$ without heating. *Caution*! Indium dissolves in $HClO_4$ with vigorous heat evolution. The resultant crystals were recrystallized three times from 60% $HClO_4$.

The hydrated salts of Al(III), Ga(III), and In(III) were dried at room temperature under vacuum just before they were converted to the corresponding Me_2SO and DMF salts.

$\mathbf{[Al(Me_2SO)_6](ClO_4)_3}$. A 100-$cm^3$ portion of triethyl orthoformate was poured into the Erlenmeyer flask containing 25 cm^3 of ethanolic solution of hydrated aluminum(III) perchlorate. Under nitrogen atmosphere the solution was stirred for 2 h, and then 10 cm^3 of fresh Me_2SO was added dropwise. Crystals of Me_2SO solvate of aluminum(III) perchlorate were

---

(1) Ishihara, K; Funahashi, S.; Tanaka, M. *Inorg. Chem.* **1983**, *22*, 2564.

(2) Ishihara, K.; Funahashi, S.; Tanaka, M. *Inorg. Chem.* **1983**, *22*, 3589.

0020-1669/86/1325-2898$01.50/0